ACS APPLIED MATERIALS & INTERFACES

Research Article

www.acsami.org

Polyvinylpyrrolidone Molecular Weight Controls Silica Shell Thickness on Au Nanoparticles with Diglycerylsilane as Precursor

Alan Vanderkooy and Michael A. Brook*

Department of Chemistry and Chemical Biology, McMaster University, 1280 Main Street West, Hamilton, Ontario, Canada L8S 4M1

Supporting Information

ABSTRACT: Several strategies have been described for the preparation of silica-encapsulated gold nanoparticles (SiO_2–AuNP), which typically suffer from an initial interface between gold and silica that is difficult to control, and layer thicknesses that are very sensitive to minor changes in silane concentration and incubation time. The silica shell thicknesses are normally equal to or larger than the gold particles themselves, which is disadvantageous when the particles are to be used for biodiagnostic applications. We present a facile and reproducible method to produce very thin silica shells (3–5 nm) on gold nanoparticles: the process is highly tolerant to changes in reaction conditions. The method utilized polyvinylpyrrolidone (PVP) of specific molecular weights to form the interface between gold and silica. The method further requires a nontraditional silica precursor, diglycerylsilane, which efficiently undergoes sol–gel processing at neutrality. Under these conditions, higher molecular weight PVP leads to thicker silica shells: PVP acts as the locus for silica growth into an interpenetrating organic–inorganic hybrid structure.

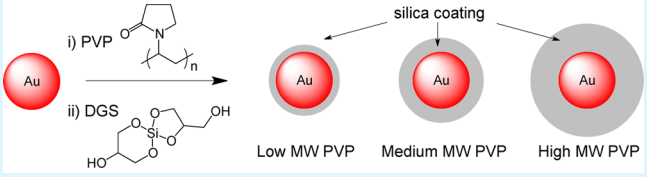

KEYWORDS: *core–shell, nanotechnology, diglyceroxysilane, AuNP, silica shell, colorimetric assay*

INTRODUCTION

Gold nanoparticles (AuNP) have received much attention in recent decades due to their physical properties, including electrochemical, catalytic, electromagnetic and colorimetric properties, which are quite distinct from bulk and atomic gold.[1,2] The colorimetric properties of AuNP arise from surface plasmon resonances (SPR) and have been the subject of a multitude of studies, in particular, due to potential applications as bioanalytical sensors.[3−5]

When AuNP are brought into close proximity by colloidal destabilization, or through molecular recognition in the case of bioassays, the plasmon resonance frequency shifts because of coupling of the electric fields between particles. The appearance of small particles changes from red to purple/blue, a color change that is the basis of many colorimetric assays based on AuNP.

The interface provided by a silica shell on silica-encapsulated AuNP (SiO_2–AuNP) provides an alternate surface chemistry to the gold to which biomolecules may be tethered. Liu et al., for example, have shown the utility of SiO_2–AuNP in aggregation-based bioanalytical assays that required the covalent attachment of single stranded DNA oligonucleotides to the shell. The particles could be aggregated using complementary oligonucleotides to hybridize and form double stranded DNA that cross-linked the particles together. The results showed a change in absorption coefficient as particles flocculated, but not a change in the wavelength of the plasmon of the particles because the silica shells were too thick (~35 nm) to permit plasmons on adjacent gold particles to interact with one another.[6−8]

Core–shell structures also have important applications in 2D and 3D assemblies such as films and lattices. The nanostructuring of SiO_2–AuNP particles allows the fabrication of materials with controlled architecture at the nanoscale, whereas classical materials can only be controlled at the molecular and macroscopic levels.[9] By manipulating the spacing of metallic nanoparticles within an assembly through the use of silica shell thickness, surface chemistry and morphology, various properties of a material can be varied including: optical and colorimetric properties, conductance and electrical properties, magnetic properties, and mechanical properties.[9,10]

The study of encapsulating AuNP in silica began in 1995 with Liz-Marzán and Philipse[11] who encapsulated AuNP by heterocoagulation with colloidal silica followed by Stöber growth[12] to cover the AuNP. SiO_2–AuNP were alternatively synthesized starting from gold cores by Liz-Marzán et al. in 1996.[13] The method involved the coating of AuNP with aminopropyltrimethoxysilane, an amine-functionalized coupling agent, which coordinated to the gold surface via the nitrogen. The methoxy groups on the other end of the molecule subsequently underwent hydrolysis/condensation to give a product that presented a vitreophilic surface on which silica could be grown by the addition of sodium silicate. Thicker silica shells could be grown by the Stöber process after transferring the particles into ethanol.

A variety of other strategies have been employed to provide alternative vitreophilic interfaces. These include using:

Received: May 9, 2012
Accepted: July 5, 2012
Published: July 5, 2012

polyvinylpyrrolidone (PVP) to prime the AuNP, avoiding the need for an initial sodium silicate shell growth;[14] different silanes to prime AuNP;[15−17] Stöber growth directly on a citrate-stabilized AuNP, thus eliminating the priming step;[18,19] ammonium-catalyzed hydrolysis and condensation of TEOS ($Si(OEt)_4$) on hydrophobic particles via a cationic micelles;[20] and reverse microemulsion-mediated synthesis.[21] For detailed reviews of such studies, the reader is referred to articles by Liu and Han[22] and by Guerrero-Martínez and co-workers.[23] The PVP priming interface was used in this study.

Recently, we demonstrated that the plasmonic changes upon aggregation of AuNP still occur in the presence of a silica shell, but the magnitude of the observed colorimetric shift is highly dependent on the thickness of the silica layer: a thin shell is required for the change to be easily observed (optimally ≤3 nm).[24] It was possible to prepare SiO_2−AuNP through two distinct methods. One was the classical ammonia-catalyzed Stöber method[12] using $Si(OEt)_4$ as precursor, which led to an increase in thickness that could be controlled by reagent concentrations and reaction time. The other process took place at neutral pH in an aqueous system using the silane precursor diglycerylsilane (DGS) (Figure 1).

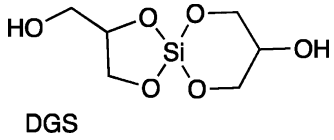

Figure 1. DGS (diglycerylsilane): a mixture of 5,6 ringed isomers with stoichiometric formula $Si(glycerol)_2$.

DGS is a relatively new silane precursor for silica shells.[25] It participates in sol−gel chemistry under biologically friendly conditions, because it undergoes hydrolysis and condensation at neutral pH[26] and the side product glycerol is tolerated well by most biological systems. Therefore, if desired, it would be reasonable to attempt the incorporation of proteins or other bioreagents into the core−shell structures described here.[27,28] In addition, the gelation time of DGS systems has been shown to be highly dependent on the ionic strength of the solution.[26] Finally, as is discussed in more detail below, the nucleophilic substitution processes leading to both hydrolysis and condensation at silicon can also be facilitated by the presence of amides.

It was found that the thicknesses of silica shells derived from DGS were highly reproducible and did not depend on either incubation time or on DGS concentration. The control of shell thickness in the size regime described here is unusual, because most shells described in the literature are much thicker (≥10 nm). Furthermore, growth processes previously examined that do lead to shells of similar thicknesses to those described here are highly dependent on conditions including concentration and time, and are thus more difficult to manage reproducibly. Understanding the ability to exercise control over shell thickness with such high fidelity and reproducibility using DGS became the focus of this work. The nature of the interaction between PVP and silica, and the dependence on the ionic strength of the kinetics of silica formation from DGS were investigated. However, the key factor is the molecular weight of the PVP used to prime the AuNP for silica deposition, which correlates directly with the thicknesses of the silica shell subsequently formed in a manner that does not significantly depend on DGS concentration or incubation time.

EXPERIMENTAL SECTION

Materials. Tetrachloroauric acid trihydrate, polyvinylpyrrolidone (PVP, MW 10 000; Lot: 099K0056, K-value[29] 16), and tetramethyl orthosilicate (TMOS) (98%) were purchased from Sigma-Aldrich. Trisodium citrate dihydrate was purchased from EM Science. Anhydrous glycerol was obtained from Fluka. Polyvinylpyrrolidone of molecular weight 3500 was purchased from Acros Organics (Lot: A0313255, K-value 12) and of molecular weight 58 000 was purchased from Alfa Aesar (Lot: 10161455, K-value 30.6).

Characterization. Transmission electron microscopy was performed using a JEOL JEM-1200EX TEMSCAN. Particle sizes and thickness of silica shells on AuNP were determined using Image J software.[30] Forty particles were measured for each treatment. The shell thickness on each particle was measured at four separate locations (at 90° increments) to eliminate bias errors due to anisotropy in the shell thicknesses. Mobility measurements were taken with a Brookhaven Instruments Corporation Zeta Potential Analyzer. UV−vis spectroscopy was performed using a Tecan Infinite M200 plate reader. Dynamic Light Scattering (DLS) data was obtained using a Melles Griot 05-LHP-928 with a high-power 35 mW helium neon laser. Measurements were averaged from three runs at 25 °C for 2 min at a wavelength of 633 nm. DLS data analysis was handled by an intensity distribution, and hydrodynamic diameter was determined using a second order cumulant algorithm.

Synthesis of Citrate-Stabilized AuNP (Citrate−AuNP). The synthesis of spherical Citrate-AuNP of diameter 16 nm, with UV−vis absorption maximum at 520 nm, was based on a previously described procedure.[18] Briefly, aqueous tetrachloroauric acid trihydrate (200 mL, 0.24 mM, 48 μmol) was heated to 80 °C. To this was added an aqueous solution of trisodium citrate dihydrate (0.94 mL, 0.34 M, 0.32 mmol). This mixture was heated at 80 °C overnight and subsequently allowed to cool to room temperature. The particles were used as prepared and characterized by UV−vis spectroscopy and transmission electron microscopy. Using the extinction coefficient given by Maye et al.,[31] the concentration of AuNP was determined to be 4 nM.

Diglyceroxysilane-Mediated Synthesis of SiO_2−AuNP. The surface modification of gold with diglyceroxysilane as the silica precursor followed our previously described procedure.[24] To three separate vials were added AuNP (20 mL). To each vial was added 400 μL of 25.6 g/L PVP in water: the molecular weight of PVP in the three vials was 3500, 10 000, and 58 000, respectively. The solutions were stirred overnight. Each sample (12 mL) was centrifuged at 16 000 g for 30 min and resuspended in water. The process was repeated once to generate PVP−AuNP.

Diglyceroxysilane (DGS) was prepared from TMOS and glycerol according to a previously described procedure involving the transesterification of TMOS with glycerol.[26] DGS was ground to a fine powder with a mortar and pestle and then dissolved in H_2O at a concentration of 10% w/v by sonicating in an ice bath for 10 min. The sample was filtered through a 0.45 μm cellulose acetate filter to remove any undissolved material.

Each sample containing a given molecular weight PVP incubation of AuNP was distributed among three vials. Fresh DGS solution was added to the PVP-AuNP to make final concentrations of 0.5, 1, and 2% w/v (DGS/H_2O). The effect of DGS concentration was examined by centrifuging and resuspending (three cycles, 16,000 g) 1 mL of each concentration of DGS after 65 min. The effect of incubation time was examined by centrifuging and resuspending (three cycles, 16 000 g) 1 mL of the 1% DGS treatments at time points 110 and 155 min.

RESULTS

Silica Shell Thickness. Gold nanoparticles were prepared using standard techniques.[18,32] Silica shells, derived from DGS, were grown on the citrate-stabilized gold surfaces that had been exposed to PVP of three different molecular weights. The

reaction was rather rapid, with silica formation reaching completion within one hour; no further changes were observed after this point (Figure 2). The majority of the particles are

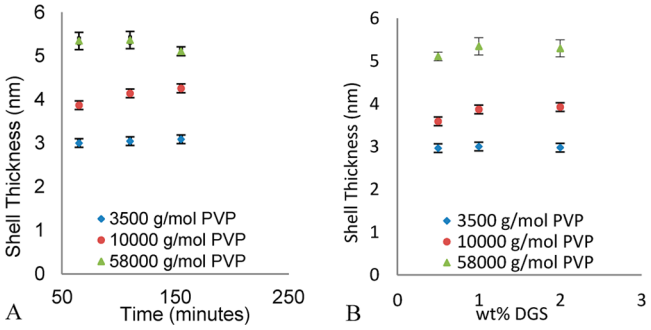

Figure 2. Dependence of silica shell thickness on molecular weight of PVP, (A) incubation time and (B) DGS concentration. Error bars represent standard error.

isolated monomeric structures, but the occasional twinned particle could be observed: note that multiparticle clusters that sometimes occur in TEM micrographs (see the Supporting Information) are a consequence of drying on the TEM grid. The thickness of the silica shells showed good correlation with the molecular weight of PVP that was used to prime the AuNP (Figure 2). Average thicknesses for particles primed with molecular weights 3500, 10 000, and 58 000 were 3.0, 4.0, and 5.2 nm, respectively. Although none of the silica shells is smooth, a higher degree of both roughness and anisotropy in the shell thickness was notable for silica shells derived from MW 58 000 PVP. As the molecular weight of the PVP increased, the deviation from spherical symmetry also increased and the distribution in shell thickness became more broad (Figure 3A) as seen in the TEM micrographs (Figure 3B and the Supporting Information, Figures S2–S19).

PVP Interface: Charge and Volume. The mobilities of the precursor Cit-AuNP were determined with a zeta potential analyzer and found to be $-2.9\ \mu s^{-1}\ V^{-1}$ cm (standard error of 0.09). The adsorption of PVP onto the AuNP led to decreased mobilities: for MW 3500, 10 000, and 58 000 Da PVP, the mobilities were −1.6, −1.4, and $-1.5\ \mu s^{-1}\ V^{-1}$ cm, respectively (standard errors of 0.07, 0.08, and 0.04, respectively). Thus, PVP displaced or neutralized some of the citrate surface charge, but this change did not depend on the molecular weight of the polymer. With further modification by silica, with shells grown using 1% DGS for 65 min, there was a significant change in surface charge only for one sample: silica on PVP-AuNP coated with 10 000 molecular weight exhibited a mobility of $-2.4\ \mu s^{-1}\ V^{-1}$ cm (standard error of 0.07), while the mobilities of particles with PVP molecular weights of 3,500; and 58,000 Da PVP exhibited mobilities of −1.8, and $-1.5\ \mu s^{-1}\ V^{-1}$ cm, respectively (standard errors of 0.07, and 0.03, respectively), comparable to their precursor particles. The UV–vis absorption spectra of all the AuNP showed a small red shift in the plasmon to 525–530 nm (see the Supporting Information, Table S1). A small absorbance red shift due to the presence of a silica shell on gold particles is a well-known phenomenon.[13]

Elemental analysis of the shells was attempted through electron dispersive X-rays (EDX). However, even using a very high sensitivity FEI Titan 80–300 TEM/STEM instrument, subtleties in the silica layer structure could not be characterized due the thinness of the sample, the overlap between signals from Si and Au, and the low efficiency of signal from nitrogen. Electron energy loss spectroscopy (EELS), using the same instrument, was compromised by contamination, likely from residual glycerol. The instrument did however shed some light on the structure of the shells. It can clearly be seen that there are no discrete changes in contrast between the edge of the AuNP and the end of the extent of the silica (see the Supporting Information, Figure S20), suggesting that the PVP and silica do not form explicitly defined layered structures.

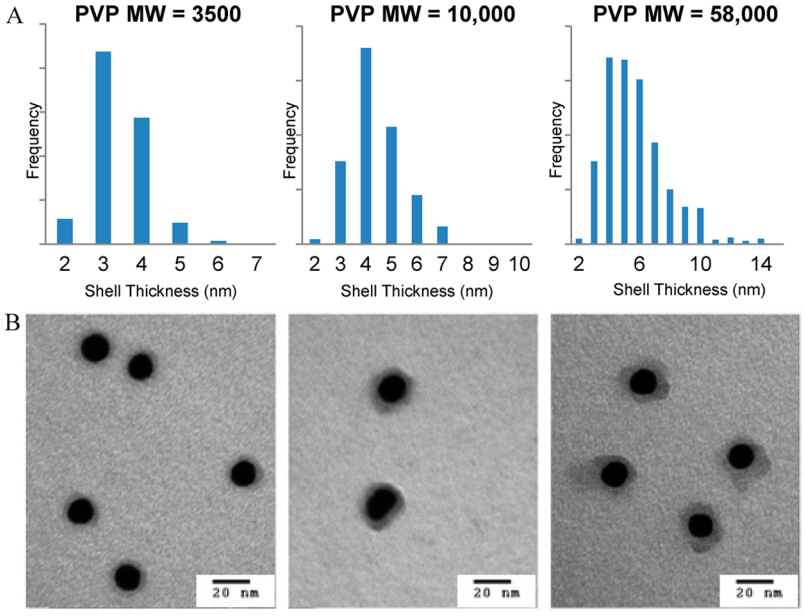

Figure 3. Distribution of silica shell thickness as a function of PVP molecular weight. (A) Distribution of shell thickness, (B) TEM micrographs of SiO_2–AuNP after incubation in 1% DGS, incubated for 110 min. Additional micrographs are included in the Supporting Information (Figures S1–S20).

dx.doi.org/10.1021/am300809q | ACS Appl. Mater. Interfaces 2012, 4, 3980–3986

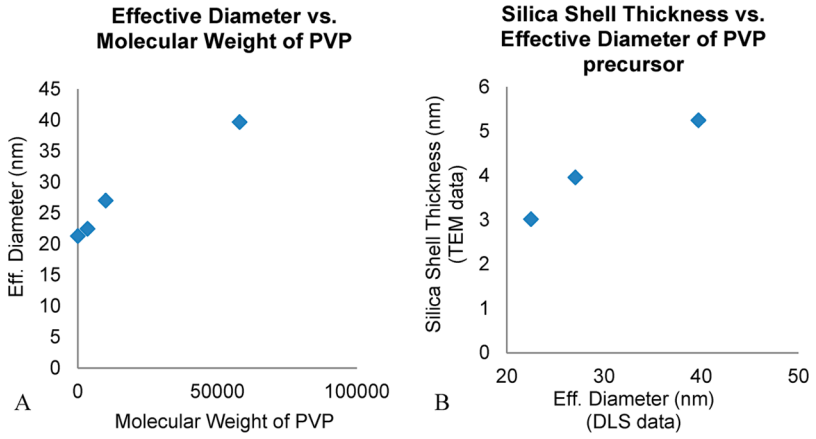

Figure 4. DLS results of PVP-coated AuNP. (A) Effective diameter of PVP−AuNP before silica coating. The point at zero represents the original citrate particles that were not treated with PVP. (B) Shell thickness of SiO_2−AuNP plotted against the effective diameter of the PVP−AuNP precursors.

Dynamic light scattering was used to compare the effective diameter of PVP-AuNP in a good solvent, which should provide better insight to the evolution of the silica shell. It was, in particular, important to establish if there was a difference between the effective diameters of the particles coated with different molecular weight PVP. The results, demonstrating a correlation with PVP molecular weight and effective diameter, can be seen in Figure 4 and in the Supporting Information (Table S2).

DISCUSSION

Electrical Double Layer. Unlike the silica precursor TEOS, with which silica shells showed steady growth over hours,[24] DGS generated shells of a given thickness at short time periods, which then stopped growing. Again unlike TEOS, for which rates of hydrolysis and condensation are highly pH dependent, DGS is much less sensitive to pH. By contrast, the condensation of silica from DGS is very sensitive to ionic strength. Gel times for silica derived from DGS were greatly reduced by the addition of salts.[26] Initially, therefore, it was hypothesized that the origin for the invariability of shell thickness with silane concentration and time were due to the kinetics of DGS sol−gel chemistry at the gold/PVP interface.

When charged particles are suspended in a solvent containing electrolytes, the concentration of ions surrounding the particles is increased relative to that of the solution, leading to an electrical double layer.[33] Charged functionalities on the surface of the particles can be due to the surface chemistry of the particles or preferential adsorption of ions, both of which may be relevant in a citrate/PVP/AuNP interface. These charges result in electrostatic repulsion between particles, which enhances colloidal stability. The primary layer of ions is surrounded by counterions from the solution, leading to an increase in the ionic strength near the surface of the particle.[33,34]

Initially, it was proposed that local charge density from partly hydrolyzed PVP[35] and from residual citrate on the AuNP surface facilitated rapid growth of silica shells from DGS: growth of the silica would terminate once the silica layer was thick enough to screen the charges. However, the electrical double layer cannot explain the control over shell thickness, since the SiO_2−AuNP themselves have an electrical double layer surrounding them which, according to the mobility measurements, is equal or greater to the electric field surrounding the PVP−AuNP. Moreover, it was not possible using DGS to directly form silica shells on (the more highly charged) citrate coated AuNP (see the Supporting Information. Figure S1). The PVP priming interface is essential to the formation of a silica coat. Furthermore, the differences in shell thickness cannot be explained by differences in surface charge, because all PVP−AuNP, regardless of molecular weight of PVP, have comparable mobilities that do not correlate with the shell thicknesses attained.

The mobilities of the SiO_2−AuNP are at least as negative as the PVP−AuNP and depend on PVP MW. It appears that the natures of the silica shell interfaces derived from different PVP molecular weights are also different. PVP with molecular weight of 10 000 produces shells with the most negative charge (−2.4 μs^{-1} V^{-1} cm). Because silanol groups are deprotonated at neutral pH,[36] the silica shell associated with PVP MW 10 000 has the highest density of silanol groups, but does not generate the thickest silica shell layer. Thus, controlled silica formation on the PVP−AuNP interface is not a consequence of surface charge.

SiO_2−PVP Interface. The PVP priming interface has been shown to be an effective method to prime AuNP for a silica coating.[14,24] The nature of the interaction between AuNP and PVP has been studied by Ullah et al. through FTIR and XPS.[37] They showed that PVP coordinates to AuNP through both the C−N and C═O groups. In FTIR, the absorption intensities of the corresponding peaks were reduced and red-shifted compared to that of pure PVP, indicating bond weakening. Furthermore, the XPS peak positions of the 1s electrons were shifted to higher energy, indicating lower electron densities on the N and O atoms. Our attempts to examine the surface using surface-enhanced Raman scattering were, as expected, unsuccessful because of the small particle size.

PVP also has a high affinity for silica, which arises from hydrogen bonding and from electrostatic interaction between negatively charged silica and PVP that contains some positive charge.[35] The structure of PVP, particularly the *N*,*N*-dialkyl substituted carboxylamide, is a frequent functionality among polymers with affinity for silica.[38] The oxygen of the carbonyl is a strong hydrogen bond acceptor and hence interacts well with strong hydrogen bond donators such as silanol groups.[39]

Nucleophilic substition at silicon can be catalyzed by silaphilic catalysts. Although fluoride is the most important

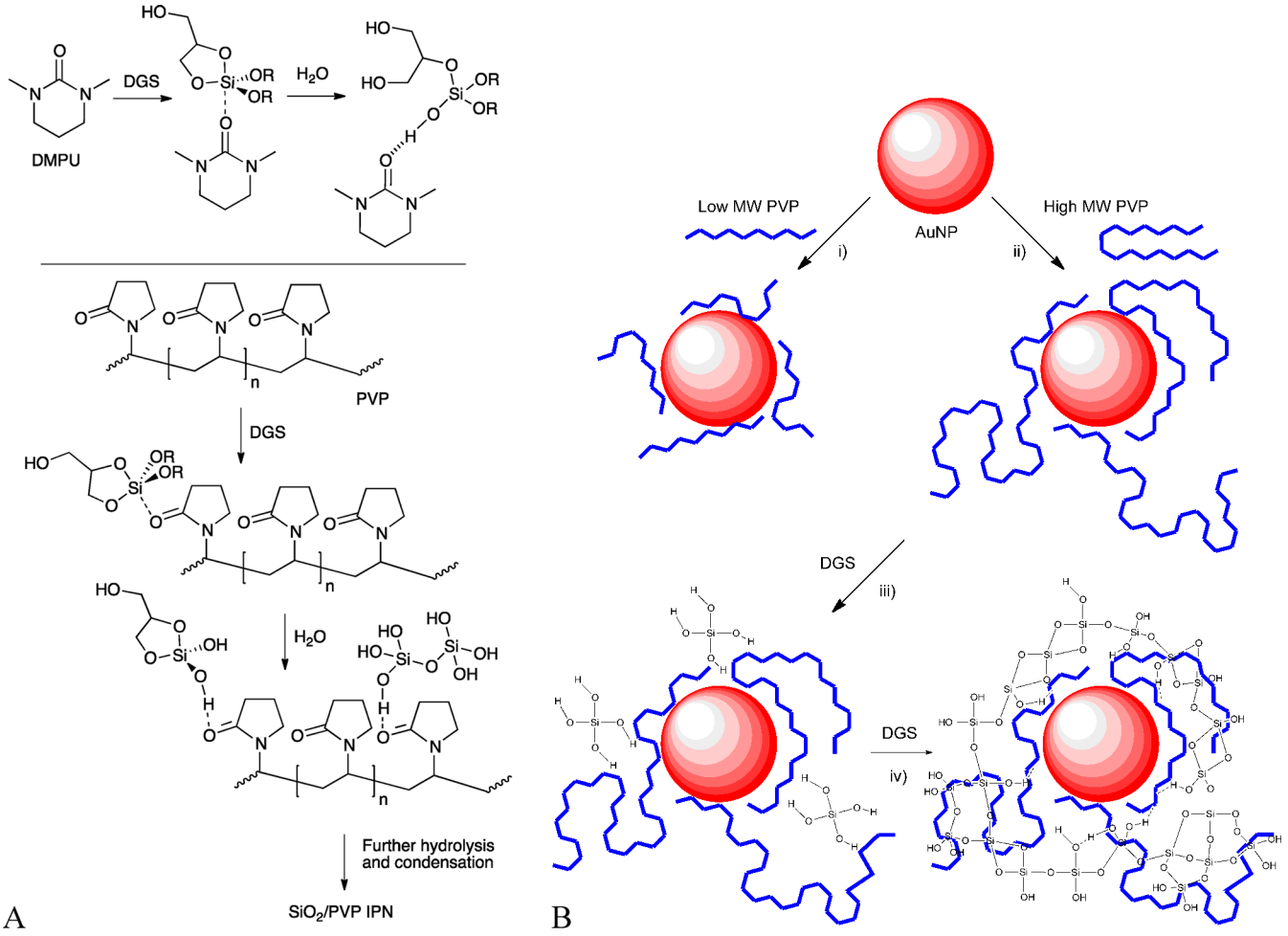

Figure 5. (A) Top: extracoordination by silaphilic catalyst DMPU facilitates hydrolysis. Bottom: proposed PVP-catalyzed process leading to a silica–PVP interpenetrating network. (B) Model showing that higher molecular weight PVP has a larger volume extending from the particle surface into solution and a larger variance in the adsorption footprint; (i) low molecular weight polymer (bold line representing PVP) adsorbed to gold; (ii) high molecular weight polymer adsorbed to gold; (iii) silanols interacting with polymer; (iv) condensed silica forming an interpenetrating network with polymer around the AuNP.

catalyst of this type, aromatic amines, and selected amides including *N*-methylpyridone and DMPU (1,3-dimethyl-3,4,5,6-tetrahydro-2(1H)-pyrimidinone)(Figure 5A).[40,41] The catalyst preactivates silicon by forming a five-coordinate complex that then succumbs to attack by a nucleophile, water or a silanol in this case. The amides on PVP are not expected to be as effective as the electron-rich urea in DMPU. Nevertheless, the high density of amide groups on the polymer may facilitate substitution at silicon when compared to bulk water. Such an interaction could explain the preferential formation of silica in the PVP layer – the primary locus of reaction – over bulk water. Once condensation starts to occur, facilitated by PVP amides, the siliceous products will be stabilized through hydrogen bonding to the amide group (Figure 5A,B).

Shell Thickness and Roughness. This method to form silica shells is unique with respect to its lack of sensitivity to silane concentration and incubation time. There is also a surprisingly high degree of control in the shell thickness (Figure 2). The thickness of the shells is well correlated with the molecular weight of the PVP used to prime the AuNP for silica deposition. Figure 2 shows that the correlation holds for all concentrations and incubation times examined. Another notable difference between the different molecular weights of PVP used is the distribution of shell thicknesses. As the molecular weight of PVP increases, a broadening of the histograms in Figure 3 occurs. In particular, the morphology of the silica around the AuNP deviates from a sphere when MW 58 000 PVP is used: some surfaces were quite rough. It is important to note that these effects do not come as a consequence of limiting concentrations of PVP, since an excess of PVP was used in all cases and had to be removed prior to shell growth via centrifugation.

The increase in the available volume (the corona) with increasing PVP MW around the AuNP for silica deposition can be seen in Figure 4. The hydrodynamic diameter of the particles increases with increasing PVP molecular weight. This relationship between molecular weight of polymers on the adsorbate dimensions has been previously reported.[42] The heights of adsorbates and the adsorption footprints of polystyrene on graphite surfaces was studied via STM by Zhang et al.[43] and both features were found to increase with increasing polymer molecular weight. Furthermore, their study shows that the distribution of the footprints broadens with increasing molecular weight. The size of a polymer's footprint has also been shown to effect the solubility of carbon

nanotubes, indicating that such effects are important in nanosystems.[44]

Both the average shell thickness and the thickness distribution can be rationalized by considering the silica shell thickness to be governed by the degree to which the PVP extends into solution, which varies as just noted, with molecular weight. With a higher molecular weight PVP there will be both a larger fraction of polymer extending into solution and a larger possibility for variance in the amount of PVP on the particle (adsorption footprint) versus the amount extending into solution. As a result, the volume of PVP available for silica deposition will also have a larger variance: that is, the PVP/AuNP surfaces will be rough.

In both this study and our previous report,[24] we have found that the silica shells derived from DGS are generally less spherical than those obtained through the Stöber method. This is particularly true when the particles were primed with PVP of molecular weight 58 000. Traditional silica precursors like TEOS lead to silica formation over hours, giving primary particles, which then aggregate and deposit on the gold surface. During the Stóber process, infilling of voids on the silica-on-gold coating leads to smooth surfaces. The process is slow and, at high pH, is an equilibrium in which silica can both deposit and dissolve.

By contrast, silica formation from DGS is exceptionally rapid, with reaction complete in much less than an hour, and operating under kinetic control: silica grows until the surfaces of PVP are covered and then stops. Thicker shells were not observed at extended reaction times, or higher concentrations of DGS, although as both time and concentration increased the incidence of secondary nucleation of purely silica particles occurred. It is proposed that the PVP corona, which will randomly extend into solution, serves as a template in which DGS is hydrolyzed and on which silica forms. In essence, the PVP acts as a template on which silica grows/precipitates leading to an interpenetrating network. Once the amide groups are no longer accessible, growth stops.

It should be noted that rarely were AuNP coencapsulated during silica shell formation to give twinned particles, as can be seen in the TEM images (see the Supporting Information, Figures S1−S20). In principle, such phenomena could limit the utility of SiO_2/AuNP in colorimetric applications. However, the number of such twins is very low and, in any event, the UV absorbance maximum shifts only slightly after shell growth (see the Supporting Information, Table S1): a red shift of AuNP upon silica coating is well-known.[13]

Given that the silica deposition requires PVP and that the molecular weight of the PVP influences the thickness and morphology of the silica shells, the key to the control over shell thickness appears to reside in the interaction between silica and PVP. High resolution TEM images (see the Supporting Information, Figure S20) suggest that the two materials do not form explicitly defined layer-by-layer architectures. From this and from evidence that PVP fills the pore volume in hybrid structures with silica, it is reasoned that the silica on SiO_2−AuNP forms an interpenetrating network with the PVP (Figure 5B).[45] Once all the available PVP is covered by silica, the DGS essentially stops reacting and thicker silica shells do not form over time. DLS data supports this proposal, because the effective diameter of the PVP−AuNP is well-correlated with the amount of silica deposited by DGS. The effective diameters of the PVP-AuNP are larger than the diameters of the SiO_2−AuNP observed in the TEM, but it is well-known that DLS overestimates particle sizes relative to TEM.[46,47] This can be seen for the citrate AuNP whose TEM diameter is 16 nm but which DLS reports as 21.3 nm.

Thus, the key differences between the sol−gel process with DGS and traditional silica precursors such as TEOS ($Si(OEt)_4$) are associated with control of the condensation process. TEOS needs to be hydrolyzed away from neutrality to gives silanols that, on oligomerization, precipitate to nucleate silica structures. That process can occur on the surface of the particles or in solution, where the silica competes to grow further on its own (secondary nucleation), or be attracted to the surface of the AuNP.[24] By contrast, DGS undergoes sol−gel processes under neutral conditions, which can be further facilitated by amide groups that catalyze both hydrolysis and condensation reactions (Figure 5A). Therefore, DGS and silanols preferentially affiliate with the PVP corona during silica formation, such that a silica/PVP interpenetrating network is formed. The network product will be stabilized by favorable hydrogen bonding interactions between free silanols and the amides. There is a unique character to our process. Other methods, such as the Stöber process, continue silica deposition after the PVP layer is covered. By contrast, DGS preferentially undergoes both hydrolysis and condensation at neutral pH within the PVP layer leading to an interpenetrating network. Once the available swollen PVP is consumed by silica formation, reaction stops leading to excellent control of shell thickness simply by choosing an appropriate MW PVP primer.

CONCLUSION

It has been shown that DGS rapidly forms silica shells on AuNP with the aid of a PVP interface. The thickness of this layer can be controlled to 3, 4, or 5 nm simply by using PVP of specific molecular weight 3500, 10 000, or 58 000, respectively: the distribution of shell thicknesses is larger and morphology of the particles is less symmetrical when molecular weight 58 000 is used. It was found that while the electrical double layer surrounding the AuNP may facilitate condensation of the silica in the vicinity of the particles, the electrical double layer does not govern the shell thickness. The shell thickness deposited was well-correlated with the effective diameters of the PVP coated particles, suggesting an interpenetrating network of organic−inorganic polymers forms. The mild conditions used to form the thin shells with high fidelity on these particles make them applicable to biologically compatible syntheses. The particles should also be applicable to colorimetric aggregation-based assays, including bioassays, and to 2D and 3D nanostructured assemblies such as films and lattices. The preparation method is particularly advantageous because it is facile and highly tolerant to changes in incubation time and concentration.

ASSOCIATED CONTENT

Supporting Information

TEM micrographs of the particles prepared from different PVP MW, comprehensive shell thickness data, UV absorption maxima, and the results of individual DLS measurements are available free of charge via the Internet at http://pubs.acs.org/.

AUTHOR INFORMATION

Corresponding Author

*E-mail: mabrook@mcmaster.ca. Phone: +1 905 525 9140 ×23483. Fax: +1 905 522 2509.

Notes

The authors declare no competing financial interest.

■ ACKNOWLEDGMENTS

We thank the Sentinel: NSERC Bioactive Paper Network and the Natural Sciences and Engineering Research Council of Canada for financial support of this research. We also thank the staff at the McMaster University Faculty of Health Science Electron Microscopy Facility and at the Canadian Centre for Electron Microscopy for their assistance, particularly Marcia Reid, Fred Pearson, and Andreas Korinek. We thank Zuohe Wang and Prof. Todd Hoare for assistance with DLS. We also thank Ferdinand Gonzaga and Yang Chen for helpful discussions.

■ REFERENCES

(1) Daniel, M.-C.; Astruc, D. *Chem. Rev.* **2003**, *104*, 293−346.
(2) Ghosh, S. K.; Pal, T. *Chem. Rev.* **2007**, *107*, 4797−4862.
(3) Zeng, S.; Yong, K.-T.; Roy, I.; Dinh, X.-Q.; Yu, X.; Luan, F. *Plasmonics* **2011**, *6*, 491−506.
(4) Zhao, W.; Brook, M. A.; Li, Y. *ChemBioChem* **2008**, *9*, 2363−2371.
(5) Rosi, N. L.; Mirkin, C. A. *Chem. Rev.* **2005**, *105*, 1547−1562.
(6) Liu, S.; Zhang, Z.; Wang, Y.; Wang, F.; Han, M.-Y. *Talanta* **2005**, *67*, 456−461.
(7) Liu, S.; Zhang, Z.; Han, M. *Anal. Chem.* **2005**, *77*, 2595−2600.
(8) Liu, S. H.; Han, M. Y. *Adv. Funct. Mater.* **2005**, *15*, 961−967.
(9) Liz-Marzán, L.; Mulvaney, P. *J. Phys. Chem. B* **2003**, *107*, 7312−7326.
(10) Wang, Z. L. *Adv. Mater.* **1998**, *10*, 13−30.
(11) Liz-Marzán, L. M.; Philipse, A. P. *J. Colloid Interface Sci.* **1995**, *176*, 459−466.
(12) Stöber, W.; Fink, A.; Bohn, E. *J. Colloid Interface Sci.* **1968**, *26*, 62−69.
(13) Liz-Marzán, L. M.; Giersig, M.; Mulvaney, P. *Langmuir* **1996**, *12*, 4329−4335.
(14) Graf, C.; Vossen, D. L. J.; Imhof, A.; van Blaaderen, A. *Langmuir* **2003**, *19*, 6693−6700.
(15) Zhu, H.; Pan, Z.; Hagaman, E. W.; Liang, C.; Overbury, S. H.; Dai, S. *J. Colloid Interface Sci.* **2005**, *287*, 360−365.
(16) Chen, M. M. Y.; Katz, A. *Langmuir* **2002**, *18*, 8566−8572.
(17) Buining, P. A.; Humbel, B. M.; Philipse, A. P.; Verkleij, A. J. *Langmuir* **1997**, *13*, 3921−3926.
(18) Mine, E.; Yamada, A.; Kobayashi, Y.; Konno, M.; Liz-Marzán, L. M. *J. Colloid Interface Sci.* **2003**, *264*, 385−390.
(19) Lee, H. B.; Yoo, Y. M.; Han, Y.-H. *Scripta Mater.* **2006**, *55*, 1127−1129.
(20) Kanehara, M.; Watanabe, Y.; Teranishi, T. *J. Nanosci. Nanotechnol.* **2009**, *9*, 673−675.
(21) Han, Y.; Jiang, J.; Lee, S. S.; Ying, J. Y. *Langmuir* **2008**, *24*, 5842−5848.
(22) Liu, S.; Han, M.-Y. *Chem.-Asian J* **2010**, *5*, 36−45.
(23) Guerrero-Martínez, A.; Pérez-Juste, J.; Liz-Marzán, L. M. *Adv. Mater.* **2010**, *22*, 1182, 1182−1195, 1195.
(24) Vanderkooy, A.; Chen, Y.; Gonzaga, F.; Brook, M. A. *ACS Appl. Mater. Interfaces* **2011**, *3*, 3942−3947.
(25) Brook, M. A.; Chen, Y.; Guo, K.; Zhang, Z.; Jin, W.; Deisingh, A.; Cruz-Aguado, J.; Brennan, J. D. *J. Sol-Gel Sci.Technol.* **2004**, *31*, 343−348.
(26) Brook, M. A.; Chen, Y.; Guo, K.; Zhang, Z.; Brennan, J. D. *J. Mater. Chem.* **2004**, *14*, 1469−1479.
(27) Voss, R.; Brook, M. A.; Thompson, J.; Chen, Y.; Pelton, R. H.; Brennan, J. D. *J. Mater. Chem.* **2007**, *17*, 4854−4863.
(28) Lin, T.-Y.; Wu, C.-H.; Brennan, J. D. *Biosens. Bioelectron.* **2007**, *22*, 1861−1867.
(29) Zeng, W.; Du, Y.; Xue, Y.; Frisch, H. L. *Mark-Houwink-Staudinger-Sakurada Constants, in Physical Properties of Polymers Handbook*, Ed: Mark, J. E., 2nd Ed., Springer, 2006, Chap. 17.
(30) Woehrle, G.; Hutchison, J.; Ozkar, S.; Finke, R. *Turk. J. Chem.* **2006**, *30*, 1−13.
(31) Maye, M. M.; Han, L.; Kariuki, N. N.; Ly, N. K.; Chan, W.-B.; Luo, J.; Zhong, C.-J. *Anal. Chim. Acta* **2003**, *496*, 17−27.
(32) Turkevich, J.; Stevenson, P. C.; Hillier, J. *Discuss. Faraday Soc.* **1951**, *11*, 55−75.
(33) Liang, Y.; Hilal, N.; Langston, P.; Starov, V. *Adv. Colloid Interface Sci.* **2007**, *134−135*, 151−166.
(34) Fischer, C.-H.; Kenndler, E. *J. Chromatogr. A* **1997**, *773*, 179−187.
(35) Esumi, K.; Oyama, M. *Langmuir* **1993**, *9*, 2020−2023.
(36) Iler, R. K. *The chemistry of silica: solubility, polymerization, colloid and surface properties, and biochemistry*; Wiley: New York, 1979.
(37) Habib Ullah, M.; Hossain, T.; Ha, C.-S. *J. Mater. Sci.* **2011**, *46*, 6988−6997.
(38) Saegusa, T. *Pure Appl. Chem.* **1995**, *67*, 1965−1970.
(39) Ogoshi, T.; Chujo, Y. *Compos. Interfaces* **2005**, *11*, 539−566.
(40) Brook, M. A. *Silicon in Organic, Organometallic, and Polymer Chemistry*, Wiley: New York, 1999. pp 115−143.
(41) Bassindale, A. R.; Taylor, P. G., Reaction Mechanisms of Nucleophilic Attack at Silicon. In *The Chemistry of Organic Silicon Compounds*, Patai, S.; Rappoport, Z., Eds., Wiley: Chichester, UK, 1989; Vol. *1*, p 839−892.
(42) Chen, L.; Ni, M; Jia, S.; Jin, X.; Ge, S; Kajiyama, T. *J. Macromol. Sci., Part B: Phys.* **1998**, *37*, 339−348.
(43) Zhang, L. S.; Manke, Z. W.; Ng, K. Y. S. *Macromolecules* **1995**, *28*, 7386−7393.
(44) Bahun, G.; Wang, C.; Adronov, A. *J. Polym. Sci., Part A: Polym. Chem.* **2006**, *44*, 1941−1951.
(45) Toki, M.; Chow, T.; Ohnaka, T.; Samura, H.; Saegusa, T. *Polym. Bull.* **1992**, *29*, 653−660.
(46) Khlebtsov, B. *Colloid J.* **2011**, *73*, 118−127.
(47) Li, Y.; Lubchenko, V.; Vekilov, P. G. *Rev. Sci. Instrum.* **2011**, 82.